Print ISSN 2682-3993
Online ISSN 2682-4000

Magnetite-Cellulose Core-Shell Nano Structure in Polymer Composite Materials for Storage Energy Applications

Sohier Mohammed Abobakr [1], Magdi Khalil [2] , Amr Mohamed Abdelghany [3]
[1] Chemical Engineering Department, Higher Institute of Engineering and Technology, New Damietta, 34517, Egypt
[2] National Water Research Center (NWRC)
[3] Spectroscopy Department, Physics Research Institute, National Research Centre, ElBehouth St., 12311, Dokki, Giza, Egypt

Abstract- The controlled design of novel materials is driving the increase of innovation in the electrical sector. Because of its numerous uses in electromagnetic interference shielding, medicine, biomedical sensing, structural engineering particularly military buildings, and soundproof buildings, solar cell, electronics devices, and so on, hybrid materials based on magnetite/cellulose nano structure are quite appealing.

Because of its multifunctionality and simplicity of integration with existing production processes, magnetite-cellulose core-shell nanocomposites or nanoparticles embedded in polymer matrices have piqued the interest of many researchers.

In this study, a new type of composite polyvinyl alcohol membranes with various concentrations of magnetite/cellulose nanostructured core shell was effectively constructed.

For all samples, the real component of the dielectric constant (έ), the dielectric loss factor (ε ″), and the ac conductivity (σac) are measured as a function of frequency from 50 Hz to 5 MHz with an applied voltage of 0.1 V using HIOKI 3532-50 LCR Hi tester. Using the ultraviolet-visible spectrum, the optical properties of thin films were studied. A decrease in dielectric constants and dielectric losses were found with increasing frequency while AC conductivity increased with increasing frequency for different concentrations of NC/MNPs at room temperature.

Because of their superior dielectric performance, these composite membranes have been found to be suitable for use in electronic devices. XRD and FTIR measurements were used to evaluate the effect of magnetite/cellulose nanostructure loading on the crystal structure of the produced composite films.

Keywords- Magnetite-Cellulose Core-Shell Nano Structure in Polymer Composite Materials for Storage Energy Applications.

I. INTRODUCTION

Recent years have seen a rise in research and industrialization of eco-friendly green composite materials due to concerns about pollution, the environment, health, safety, and the depletion of fossil fuel resources. A green substance that is abundantly found in nature, inexpensive, non-toxic, biodegradable, and biocompatible is cellulose. Cellulose ($C_6H_{10}O_5$) is considered to be a natural polymer constructed of D-glucose units connected by glycosidic linkages. Because there are many hydroxyl groups in this structure, linear polymeric chains with a high polar surface are produced [1]. There are numerous processes used to create nanocellulose, including acid hydrolysis, ultrasonic technology, and enzymatic hydrolysis [2]. The most used technique is acid hydrolysis. This process is quick and simple and yields nanocellulose with superior qualities. Research has indicated that nanocellulose generated via acid hydrolysis possesses a higher crystallinity index in comparison to nanocellulose generated using alternative techniques. Furthermore, the nanocellulose generated by acid hydrolysis has a smaller dimension. These are the justifications behind the study's decision to use an acid hydrolysis approach to produce nanocellulose. [4,16,17]

The specific characteristics of nanocellulose are determined by the extraction, purification, and sourcing processes. Because of their nano size and the hydroxyl groups that exist on their surface, which can be avoided by surface modification, different types of nanocellulose have specific characteristics such chemical reactivity and high mechanical properties of films [6,18].

A number of advanced applications for NCC and NFC that have been demonstrated include optically transparent materials, coating films, drug supply, aerogels, biomedical materials, sensors, energy harvesters, rheology modifiers, filtration textiles, electronics, composites, packaging paper and board,

Print ISSN 2682-3993
Online ISSN 2682-4000

oil and gas, medical and healthcare [3]. Energy storage systems furthermore employ mesoporous and macroporous nanocellulose particles. The properties of the cellulose, including its crystallinity, porosity, pore dispersion, and pore-size distribution, determine how the cellulose beads function as electrodes that supplement traditional supercapacitors and batteries [3].

Paper sheets or regenerated cellulose (cellophane) have been used as dielectric materials for electrical insulation since cellulose's electrical characteristics have been carefully studied [1]. Lately, materials that are electrically conductive, semiconducting, and insulating have been created using cellulose nanofibers as a matrix. One of the best methods to understand the structure of cellulose is to look at how it is used in electrical applications by looking at the dielectric constant and dielectric loss as a function of frequency.

The creation of hybrid organic/inorganic composites is of interest to scientists. The combination of various organic and inorganic ingredient properties, such as high flexibility, dielectric, and piezoelectric qualities provided by an organic component like nanocellulose and the potential for magnetic and electric properties from an inorganic component, gives hybrid multifunctional materials advantages. Thanks to the controlled surface modification of nanocellulose, it is now possible to produce electrical hybrid inorganic-organic nanomaterials. For this kind of research, different magnetic particles were used to nanocellulose. By using magnetic resonance imaging and inductive heating, magnetite inclusion in NC facilitates the specific targeting, identification, and possible treatment of cancer tissue.[6]

One of the applications of hybrid organic/inorganic composites is that they serve as ion-selective membranes. The ion-selective electrodes offer quick, easy, affordable, and dependable ways to identify heavy metal ions on-site. The field of hybrid materials is quite broad, open, and promising; it is worth exploring new avenues to enhance their applicability [7].

Materials known as nanocomposites are created by combining two different substances: an additive (such as nanofibers, nanometals, nanofiber oxide, or any other material) with a polymer matrix.

Lightweight nanocomposites with high specific strength, tight linking, high ionic conductivity, biodegradability, semi-crystalline polymers, fibers, and biologically produced polymers are all necessary for piezoelectric nanocomposites. The characteristics mentioned above describe polyvinyl alcohol (PVA) [8].

In the present study, magnetite nanoparticles (Fe_3O_4) and nano-cellulose were selected as naturally renewable green dielectric materials. The hybrid materials based on magnetite/cellulose nano support polymeric nanocomposite to make membrane film.

II. EXPERIMENTAL

A. Materials

The materials were deionized water, hydrogen peroxide (4% v/v), sodium hydroxide (1 M), sulfuric acid (98%), and sugarcane bagasse (SCB) from a neighboring juice shop (Juice Box Store; Egypt) [9].

B. Preparation of NC/Fe_3O_4 Core Shell

According to the published process [**9**], by hydrolysis of cellulose that was separated from sugarcane bagasse with acid (H_2SO_4), nanocellulose (NC) was created and separated centrifuged from the liquid phase and rinsed with deionized water until pH was achieved 5.5 is the value. The sulfate ions were subsequently neutralized and eliminated by dialyzing the solution for five days. To ensure the generated nano-cellulose is homogeneous, the neutral colloidal suspension was sonicated for 30 minutes.

Fe(III) and Fe(II) ions were co-precipitated in an ammonia-rich aqueous solution containing NC to create the functionalized nanocellulose. 200 mL of distilled water and 1.5 g of NC were combined and left for 10 minutes. A 2:1 combination of $FeCl_3$ -$6H_2O$ and $FeSO_4$ -$7H_2O$ was heated to 60 ^oC in order to provide sources of ferrous and ferric ions. Chemical precipitation was accomplished by adding 8.0M of ammonia solution dropwise, vigorously spinning, and keeping the pH at 10. After precipitation, an orange-colored suspension gave way to a black precipitate. The mixture was stirred while it was cooled to room temperature following a 4-hour incubation period at 60 ^oC. Following numerous distilled water washes, the final NC/Fe_3O_4 particles were dried.

Print ISSN 2682-3993
Online ISSN 2682-4000

C. Preparation of PVA Film Incorporated with NC/Fe_3O_4 Core Shell

A concentration of 5 g/100 mL PVA (Mw = 89,000-98,000) was dissolved in deionized water using a magnetic stirrer. A heated plate set at 90 degrees Celsius and an overhead mechanical mixer were used to make the nanocomposite film. For thirty minutes, different NC/Fe_3O_4 concentrations (2%, 3%, 4%, and 6% w/v) were introduced and agitated at 200 rpm. The resulting hydrogel mixture was carefully poured into a 14-centimeter diameter Petri plate. After using a spirit level to level out the petri dish and ensure that the hydrogel was distributed evenly, the dish was left in the room for half an hour.

D. Structural characterization

X-Ray Diffraction: A CuK radiation excitation source (= 1.541) was used in conjunction with a scanning angle of 30 to 80° at a scan rate of 5°/min to perform XRD experiments on a Shimadzu LabX XRD-6000. Fourier-transform infrared spectroscopy: The chemistry of NCs and the nanohybrid film was examined using a Perkin Elmer S-100 FT-IR spectrometer, which was scanned from 5000 to 500 cm-1 (Transmission%). Scanning electron microscopy (SEM) was applied to study the morphology of NCs and JSM-6510, JEOL, Ltd. micrographs of the samples were acquired.

E. Electrical Properties measurements

The produced films were positioned between the two electrodes, and the electrical characteristics of the films were examined using a HIOKI 353250 LCR Hi tester at 298 K with a frequency range of 0.1 Hz to 5 MHz and an applied voltage of 0.1V. This study computed the dielectric constant ′, dielectric loss ″, and electrical conductivity by measuring dissipation factor D, capacitance Cp, and resistance Rp. The equation from the measured capacitance at all frequencies and 298 K in our tests was used to derive the real component of the dielectric constant [1,12]:

$$\varepsilon' \text{ ¼ } Cpd=\varepsilon oA \quad (1)$$

where ε o is the free-space permittivity, A is the area of the film under inspection and d is the thickness of the thin films.
The dielectric loss was computed using the relationship

$$\varepsilon'' = \varepsilon' \tan\theta \quad (2)$$

The observed resistance values for the film under test were used to determine the ac conductivity's frequency dependency, or σ ac.
The relation :

$$\sigma ac \text{ ¼ } d=Rpa \quad (3)$$

was used to compute the ac electrical conductivity. In this relationships, a is the film's cross-section area, Rp represents the saw film resistance, and d is its thickness.

Figure 1. A HIOKI 353250 LCR Hi tester on a frequency range of 0.1 Hz to 5 MHz with a 0.1V applied voltage**.**

Print ISSN 2682-3993
Online ISSN 2682-4000

III RESULTS AND DISCUSSION

A. Structural characterization

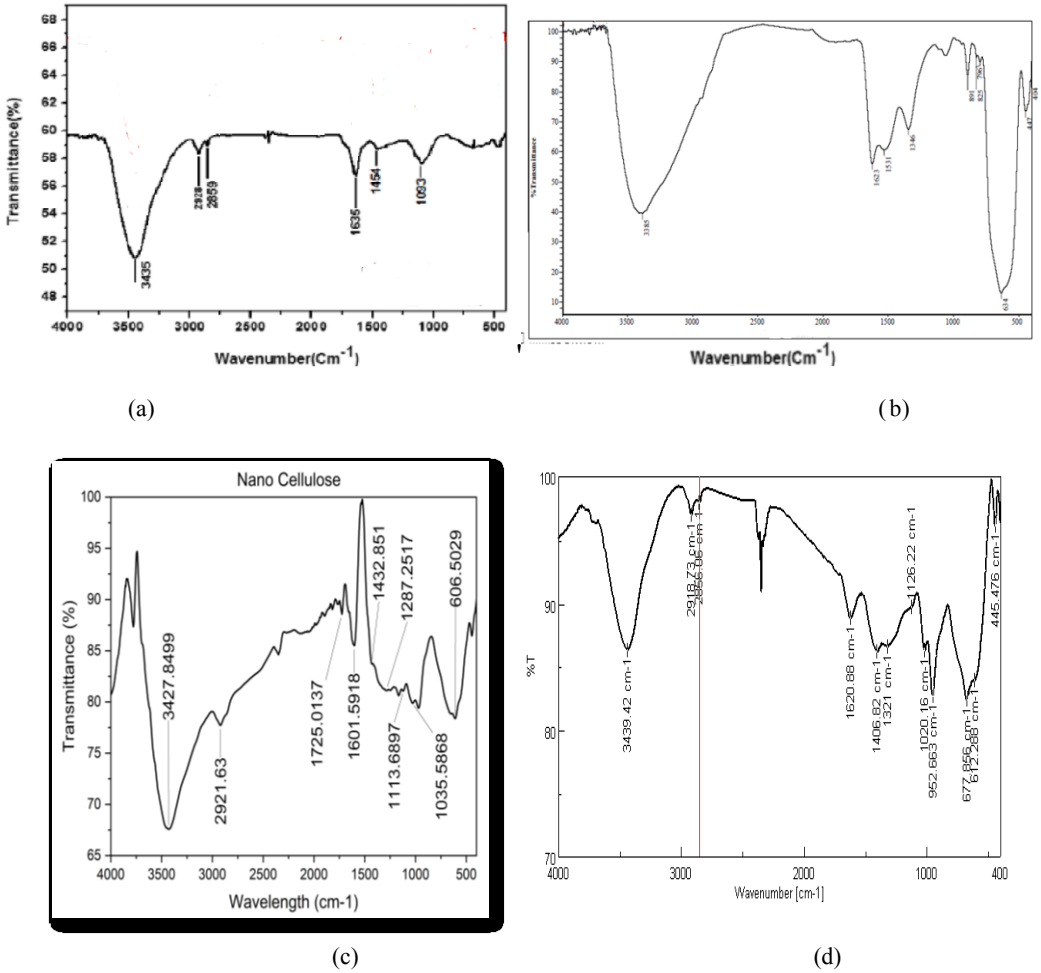

(a) (b)

(c) (d)

Figure 2. FT-IR spectra: (a) PVA; (b) MNPs; (c) NC and (d) PVA Film Incorporated with NC/Fe_3O_4 Core Shell.

i. FT-IR spectra

The different functional groups were identified using FTIR analysis, as shown in Figure 2, in an effort to comprehend PVA, NC, and Fe3O4's intermolecular interactions better. The FT-IR absorption spectra of pure PVA polymer (Fig. 2 (a) exhibit distinctive bands associated with the polymer's functional groups. The O-H stretching vibrations from PVA's intermolecular and intramolecular hydrogen bonds are responsible for the broad bands centered at 3435 cm-1 [12].. The hallmark bands of asymmetric and symmetric C-H stretching are peaks at 2928 and 2859 cm-1, respectively. C=O and C-O-C stretching vibrational bands at 1635 and 1093 cm-1, respectively.

The absorption peaks linked to O-H stretching at 3439 cm-1 were slightly broadened and amplified as a result of the PVA inserting it self into the core shell of NC-MNPs. This may be explained by the intermolecular contact between the NC-MNPs' core-shell and the hydroxyl groups in PVA. With a little rise in peak intensity, the bands for C-H and CH2 asymmetric stretching at 2918.73 and 2856.06 cm-1, respectively, remained constant throughout the combined films. The minor alterations seen in the composite films might be accounted for by the chemical interactions between NC - MNPs, which served as a binder between PVA and Fe3O4, and the functional groups of the PVA matrix. The successful integration of NC and Fe3O4 nanoparticles in PVA was confirmed by the existence of two

Print ISSN 2682-3993
Online ISSN 2682-4000

extra absorption bands at 677.8–61.28 and 445 cm^{-1} in just the hybrid films. Fe–O–C bonds between iron oxides and polymers were identified as the source of these absorption bands. The presence of Fe–O bonds is indicated by the fingerprint of Fe_3O_4 in the region of 677.8–612.28 cm^{-1} [6]. The appearance of the individual materials' characteristic fingerprints proved the effective synthesis of the ternary composite film.

ii. X-ray diffraction (XRD)

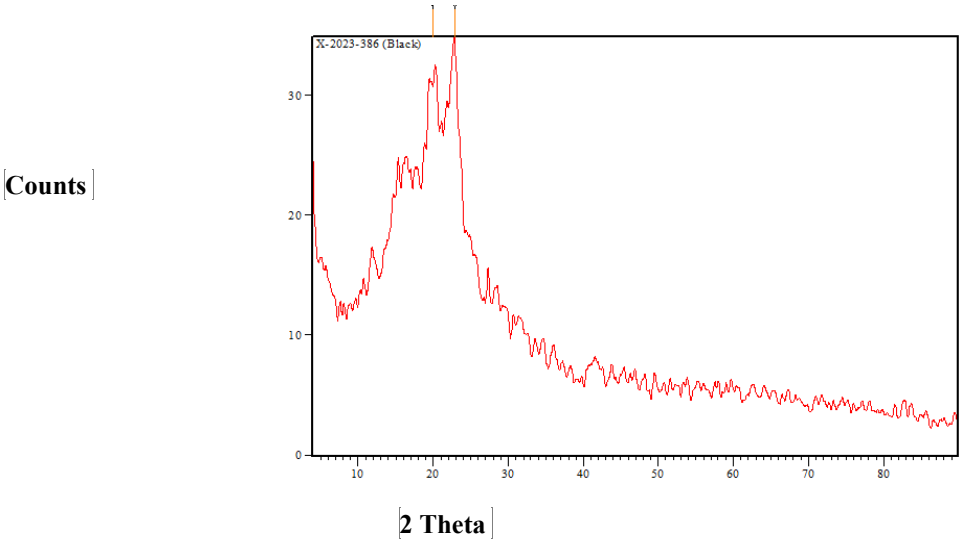

Figure 3. X-ray diffraction pattern of PVA Film Incorporated with NC/Fe3O4 Core-shell

Table 1 XRD results of PVA Film Incorporated with NC/Fe3O4 Core shell from the most intense peak.

Pos. [°2θ]	d-spacing [Å]	Height [cts]	FWHM Left [°2θ]	Rel. Int. [%]	h	k	l
19.9009	4.46154	9.16	0.9446	62.25			
22.8812	3.88671	14.71	0.7085	100.00			

Figure 3 displays the diffraction pattern of the hybrid film containing polymeric and magnetic nanoparticle components. The chemical interactions between nanoparticles and the PVA matrix are reflected in the fingerprints (42). Strong filler-matrix bonding was established in the PVA Film Incorporated with NC/Fe_3O_4 core-shell due to the higher concentration of hydroxyl groups and PVA matrix. The peaks of PVA crystalline diffraction are located at 2θ = 19.9° and 22.8°. The crystalline structure of the orthorhombic PVA lattice is indicated by the peak located at 2θ = 19.9 o. In contrast, the PVA peak intensity in the hybrid films significantly decreased as a result of the nanoparticle integration. Changes in NC/Fe_3O_4 Core-shell loadings lead to differences in crystal structure and phase purity, which are examined using X-ray diffraction. A typical cellulose II structure can be seen in the pure NC diffractogram, which has conspicuous doublets at 20 and 22 o and a low-intensity peak at 12 ° (38, 39). A similar pattern was noted by Lani et al. in (40). The fingerprint shows the presence of Fe_3O_4 in the film at 2 = 30 o, 35.6 °, 43.2 °, 57.2 °, and 63 °.

In the Fe_3O_4/NC core-shell, the characteristic signals at 30 °, 35.6 °, 43 °, 57.2 °, and 63 ° show the presence of pure Fe_3O_4 with a spinel structure (41). These matched the crystal planes (311), (220), (511), (400), and (440) based on the reference standard peak (JCPDS no. 019-0629) (43,44). The (002) crystallographic plane is where the NC/Fe_3O_4 Core-shell's crystalline peak is located at 2 = 22.6 °. The other minor peaks, on the other hand, faded as a result of Fe ions' hydroxyl group chemisorption to produce Fe-OH molecules. The strength of PVA peaks reduced steadily as the NC/Fe_3O_4 Core-shell content of the PVA chains climbed.

Print ISSN 2682-3993
Online ISSN 2682-4000

B. Electrical properties of the prepared NC -NMPs / PVA composite thin films

In a temperature range of 298 K, the electrical characteristics of NC -NMPs /PVA composite films at varied concentrations of 0.02,0.03,0.04, and 0.06 of NC -NMPs Core-Shell were examined.
Figure 2 depicts the fluctuation of σdc with log frequency for NC-NMPs/PVA composite thin films.

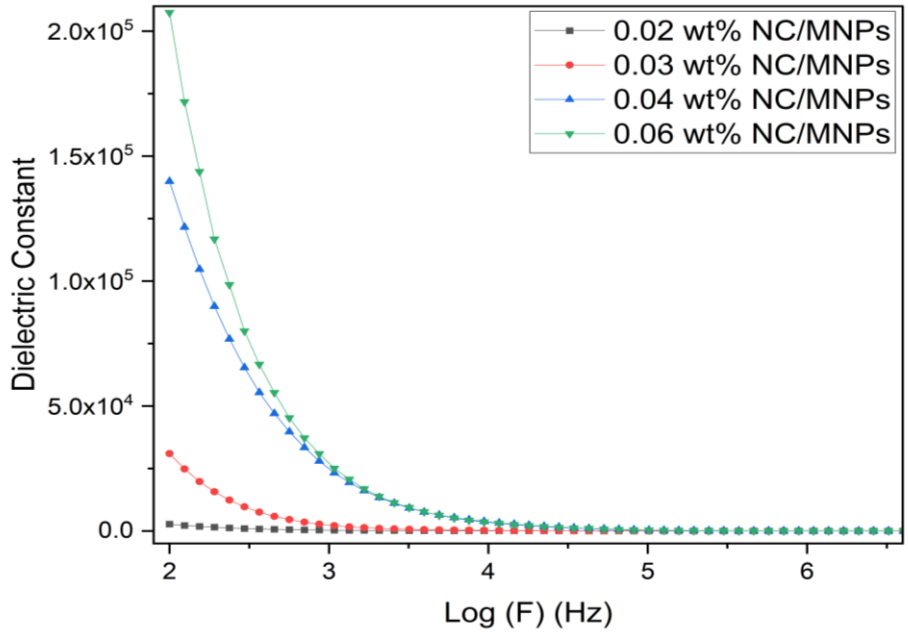

Figure 4. Variation of dielectric constant with the frequency for different concentrations of NC/MNPs at room temperature.

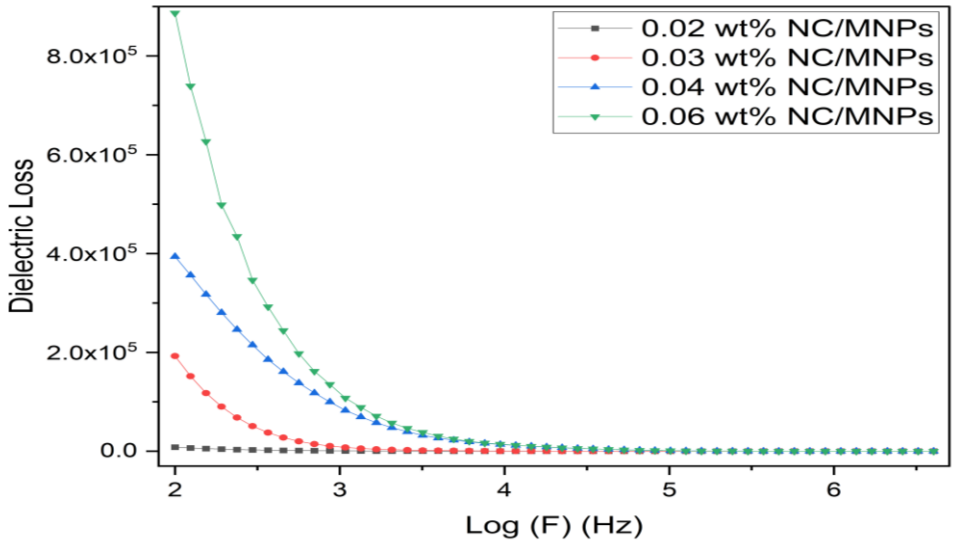

Figure 5. Variation of dielectric loss with the frequency for different concentrations of NC/MNPs at room temperature.

Plotting dielectric characteristics against frequency for different NC/MNP concentrations at room temperature is shown in Figures 4 and 5. Nanocomposites have significant dielectric constants and dielectric losses at low frequencies, but as the frequency rises, their properties rapidly drop because electric dipoles have more time to adapt to the electric field before it changes direction. However, because of the time constraints allowed for electric dipole compatibility, the dielectric loss and dielectric constant of polyvinyl alcohol-based membrane nanocomposites are decreased at high frequencies. Because of an increase in charge carrier density in the polyvinyl alcohol-NC/MNPs

Print ISSN 2682-3993
Online ISSN 2682-4000

composite matrix, they grow as NC/MNPs nanoparticle concentrations rise and eventually reach a constant value at a specific frequency.

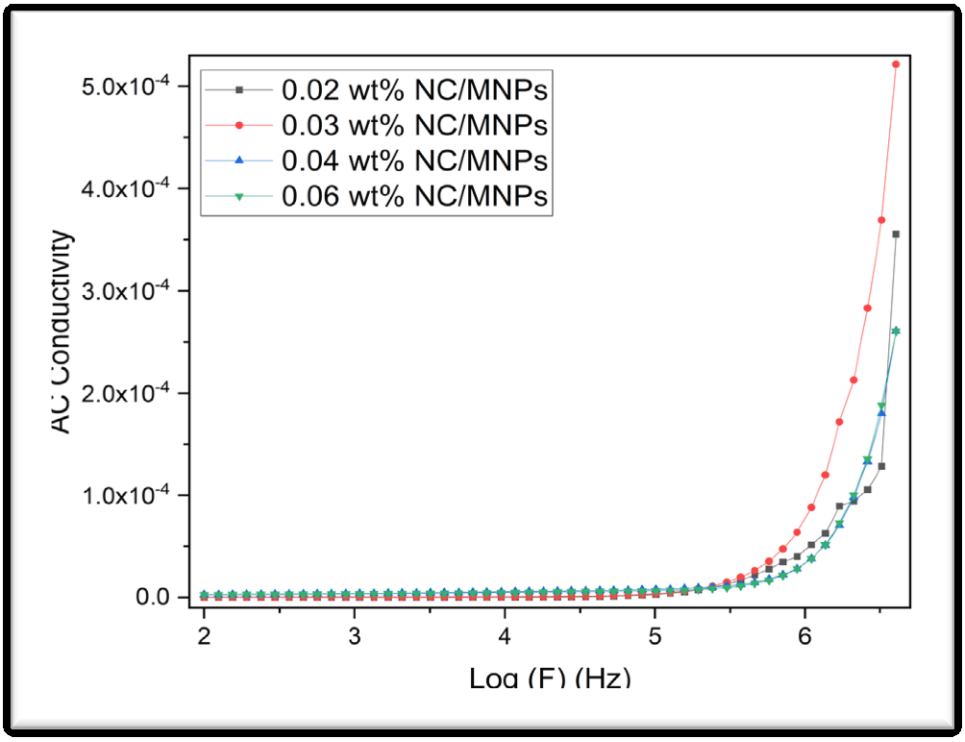

Figure6. Variation of A.C conductivity with the frequency for different concentrations of NC/MNPs at room temperature.

Figure 6 represents the changes in A.C conductivity and frequency for NC -NMPs /PVA composite films at various concentrations of NC -NMPs Core-Shell of 0.02,0.03,0.04, and 0.06. Because of interfacial polarization, conductivity increases with increasing frequency. Furthermore, with an increase in NC/MNPs, conductivity for (NC -NMPs /PVA composite film increases. The increase in electrical conductivity with increasing NC/MNPs is related to the increased charges carried in the PVA blend.

IV CONCLUSION

This work presents a novel strategy for energy storage applications in the realm of polymer composites by combining cellulose and magnetite core-shell nanostructures. The findings have potential applications in the energy and materials science fields. Comprehensive techniques like XRD, FTIR, and SEM analyses were employed in the study to characterize the composite materials and illustrate their properties. The ability of these materials to absorb electromagnetic waves in infrared radiation (IR) is a notable advancement in the application of such materials. The research showed enhanced insulating and conductive properties of composite membranes, making them suitable for use in electronic devices, military buildings, and soundproof buildings.
A greener substitute for conventional industrial materials is offered by the combination of cellulose, a renewable and biodegradable resource, with magnetite. With possible uses in energy storage and electronics, the study offered insightful information about the creation of novel composite materials.

Print ISSN 2682-3993

Online ISSN 2682-4000

REFERENCES

[1] A.M. Abdel-karim, A.H. Salama, M.L. Hassan. Electrical conductivity and dielectric properties of nanofibrillated cellulose thin films from bagasse. *J Phys Org Chem*. (2018); e3851. https://doi.org/10.1002/poc.3851

[2] K. Plermjai1,etl. Extraction and Characterization of Nanocellulose from Sugarcane Bagasse by Ball-milling-assisted Acid Hydrolysis. *International Conference on Science and Technology of Emerging Materials.* AIP Conf. Proc. 2010, 020005-1–020005-7; https://doi.org/10.1063/1.5053181

[3] A. Abdoulhdi, O. Borhana, etl. Micro- and Nanocellulose in Polymer Composite Materials: A Review. Polymers (2021), 13, 231. https://doi.org/10.3390/polym13020231

[4] W. T. Wulandari, A. Rochliadi and I.M. Arcana. Nanocellulose prepared by acid hydrolysis of isolated cellulose from sugarcane bagasse. Materials Science and Engineering 107 (2016) 012045 doi:10.1088/1757

[5] T. S. Anirudhan and S. R. Rejeena, Selective adsorption of hemoglobin using polymer-grafted-magnetite nanocellulose composite. Carbohydrate Polymers 93 (2013) 518– 527.

[6] L. Nalbandian etl. Magnetic Nanoparticles in Medical Diagnostic Applications: Synthesis, Characterization and Proteins Conjugation. Current Nanoscience. , (2016) V.12, Issue 4. DOI: 10.2174/1573413712666151210230002

[7] Polymers and Polymeric Composites: A Reference Series. http://www.springer.com/series/15068

[8] M. Qayssar Jebur, A. Hashim and A.Majeed Habeeb**.** Structural, A.C electrical and Optical properties of (Polyvinyl alcohol–Polyethylene Oxide–Aluminum Oxide) Nanocomposites for Piezoelectric Devices**.** *Egypt.J.Chem.* (2019) Vol. 62, Special Issue (Part 2), pp. 719- 734

[9] I. Abdo Nabiha, M. Tufik. Yasser, M. Abobakr Sohier . A comparison of nano-celluloses prepared with various terms of time and sulfuric acid concentration from bagasse derived cellulose: Physicochemical characteristics and process optimization. Current Research in Green and Sustainable Chemistry 6 (2023) 100365

[10] M.Qayssar Jebur , H. Ahmed, A. Habeeb. Majeed. Structural, Electrical and Optical Properties for (Polyvinyl Alcohol–Polyethylene Oxide–Magnesium Oxide) Nanocomposites for Optoelectronics Applications . Transactions on Electrical and Electronic Materials. https://doi.org/10.1007/s42341-019-00121-x.

[11] T.S. Anirudhan, S.R. Rejeena. Selective adsorption of hemoglobin using polymer-grafted-magnetite nanocellulose composite**.** Carbohydrate Polymers *93 (2013) 518– 527*

[12] *H. M. Zidan1, N. A. El-Ghamaz, A. M. Abdelghany, A. Lotfy*. Structural and Electrical Properties of PVA/PVP Blend Doped with Methylene Blue Dye. *Int. J. Electrochem. Sci.,* 11 (2016) 9041 – 9056, doi: 10.20964/2016.11.08

[13] T. S. Anirudhan, S. R. Rejeena, and J. Binusree. Adsorptive Separation of Myoglobin from Aqueous Solutions Using Iron Oxide Magnetic Nanoparticles Modified with Functionalized Nanocrystalline Cellulose. Journal of Chemical & Engineering Data (2013). dx.doi.org/10.1021/je400088g | J. Chem. Eng.

[14] W. T. Wulandari, A. Rochliadi and IM. Arcana. Nanocellulose prepared by acid hydrolysis of isolated cellulose from sugarcane bagasse. Materials Science and Engineering 107 (2016). 012045 doi:10.1088/1757-899X/107/1/012045.

[15] S. Widiarto1,2,, S. D. Yuwono2, A. Rochliadi1 and I. M. Arcana. Preparation and Characterization of Cellulose and Nanocellulose from Agro-industrial Waste - Cassava Peel. Materials Science and Engineering 176 (2017) 012052 doi:10.1088/1757-899X/176/1/012052

[16] J. Aleksandra etl. Structural Characterization of Nanocellulose/Fe3O4 Hybrid Nanomaterials. Polymers (2022), 14, 1819. https://doi.org/10.3390/polym14091819.

[17] P. Kaur. etl. Nanocellulose: Resources, Physio-Chemical Properties, Current Uses and Future Applications. Frontiers in Nanotechnology (2021). doi: 10.3389/fnano.2021.747329.

[18] T. Djalal etl. Nanocellulose: From Fundamentals to Advanced Applications. Frontiers in Chemistry (2020)V8 .